A mechanism of macroscopic (amorphous) aggregation of the tobacco mosaic virus coat protein

ARTICLE *in* THE INTERNATIONAL JOURNAL OF BIOCHEMISTRY & CELL BIOLOGY · NOVEMBER 2003

Impact Factor: 4.05 · DOI: 10.1016/S1357-2725(03)00106-7 · Source: PubMed

PERGAMON The International Journal of Biochemistry & Cell Biology 35 (2003) 1452–1460

IJBCB

www.elsevier.com/locate/ijbcb

A mechanism of macroscopic (amorphous) aggregation of the tobacco mosaic virus coat protein

Elvira R. Rafikova [a], Boris I. Kurganov [b], Alexander M. Arutyunyan [a], Stanislav V. Kust [a], Vladimir A. Drachev [a], Evgeny N. Dobrov [a,*]

[a] *A.N. Belozersky Institute of Physico-Chemical Biology, Moscow State University, Moscow 11999, Russia*
[b] *Bach Institute of Biochemistry, Russian Academy of Sciences, Leninsky pr. 33, Moscow 119071, Russia*

Received 19 December 2002

Abstract

To gain more insight into the mechanisms of heating-induced irreversible macroscopic aggregation of the tobacco mosaic virus (TMV) coat protein (CP), the effects of pH and ionic strength on this process were studied using turbidimetry, CD spectroscopy, and fluorescence spectroscopy. At 42 °C, the TMV CP passed very rapidly (in less than 15 s) into a slightly unfolded conformation, presumably because heating disordered a segment of the subunit where the so-called hydrophobic girdle of the molecule resides. We suppose that the amino acid residues of this girdle are responsible for the aberrant hydrophobic interactions between subunits that initiate macroscopic protein aggregation. Its rate increased by several thousands of times as the phosphate buffer molarity was varied from 20 to 70 mM, suggesting that neutralization of strong repulsive electrostatic interactions of TMV CP molecules at high ionic strengths is a prerequisite for amorphous aggregation of this protein.

Keywords: Tobacco mosaic virus coat protein; Aggregation; Denaturation; Kinetics; Ionic strength

1. Introduction

Mature, relatively ordered protein aggregates called amyloid fibrils, or plaques have been implicated in pathogenesis of prion infections and amyloid diseases for over several recent years, which constitute the whole history of their molecular biological studies. However, newer evidence suggests that some nonfibrillar intermediate products, rather than mature amyloid fibrils, play the major role in their pathogenesis (Conway et al., 2000; Hartley et al., 1999; Lambert et al., 1998). Interestingly, under certain conditions, amyloid fibrils can originate from misfolding of normal proteins and peptides, not associated with any pathology (Chiti et al., 1999; Fandrich, Fletcher, & Dobson, 2001; Guijarro, Sunde, Jones, Campbell, & Dobson, 1998). In April 2002, a study from Prof. C.M. Dobson's laboratory was published demonstrating that prefibrillar (amorphous and granular) aggregates of fragments of "normal" proteins, but not the mature fibrils, produced cytotoxic effects in cell cultures (Bucciantini et al., 2002). These results implicate amorphous "nonspecific" protein aggregates

Abbreviations: CP, coat protein; PB, K^+/K^+ phosphate buffer; PVX, potato virus X; TMV, tobacco mosaic virus; ToMV, tomato mosaic virus

*Corresponding author. Tel.: +7-95-939-5008; fax: +7-95-939-3181.
E-mail address: dobrov@belozersky.msu.ru (E.N. Dobrov).

1357-2725/03/$ – see front matter © 2003 Elsevier Science Ltd. All rights reserved.
doi:10.1016/S1357-2725(03)00106-7

in pathogenesis of a variety of diseases (including neurodegenerative ones) for which the authors coined the term "protein misfolding diseases" (Bucciantini et al., 2002).

The coat protein (CP) from wild-type tobacco mosaic virus (TMV) is a convenient model system for studying this type of aggregates, called by different authors non-native (Wetzel, 1994), disordered (Fink, 1998), amorphous (Bucciantini et al., 2002; Fink, 1998; Kopito, 2000), macroscopic (Ganesh, Zaidi, Udgaonkar, & Varadarajan, 2001; Orlov et al., 2001), or nonspecific (Orlov et al., 2001). As shown in our previous studies (Abu-Eid, Kust, Makeeva, Novikov, & Dobrov, 1994; Arutyunyan, Rafikova, Drachev, & Dobrov, 2001; Kurganov, Rafikova, & Dobrov, 2002; Orlov et al., 1998, 2001), when TMV CP is heated in a phosphate buffer (PB) ranging from 20 to 150 mM in molarity and from 7.0 to 8.0 in pH, the turbidity of its solution measured as absorbance at $\lambda > 305$ nm rises dramatically in a highly reproducible manner. The rate of the process and final turbidity can be easily regulated by altering the TMV CP concentration, ionic strength, and temperature. In the present work, to gain more insight into the possible mechanisms of temperature-induced irreversible macroscopic aggregation of this protein, we studied the effects of different factors on this process.

2. Materials and methods

2.1. Purification of viruses and CP preparation

Wild-type (strain U1) TMV and its ts21–66 mutant (Dobrov, Abu-Eid, Solovyev, Kust, & Novikov, 1997) were obtained as described elsewhere (Dobrov et al., 1997). Strain U1 and ts21–66 coat proteins were isolated by the acetic acid method (Fraenkel-Conrat, 1957). The same methods were employed for isolating tomato mosaic virus (ToMV) and its CP. Potato virus X (PVX) was purified as described by Goldshtein et al. (1990) and its CP was isolated by the LiCl method (Goodman, 1975).

The CP preparations were stored at concentrations of 3–5 mg/ml in 5 mM phosphate buffer (PB; pH 8.0) at +4 or −20 °C. The protein concentration was measured by UV spectroscopy using the extinction coefficient $\varepsilon_{280}^{0.1\%}$ of 1.20 for the PVX CP (Goodman, 1975) and of 1.30 for U1, ts21–66, and ToMV CPs (Orlov et al., 2001).

2.2. UV spectroscopy

The absorption spectra, the kinetics of CP macroscopic aggregation at constant temperatures (42 or 52 °C), and the stepwise heating ("melting") curves were recorded in 0.5 or 1 cm cuvettes using a UV-Vis Specord spectrophotometer (Carl Zeiss, Germany) or an SLM-Aminco DW-2000 (USA) instrument. The protein concentration in these experiments was varied from 20 to 400 μg/ml (Orlov et al., 2001). A cuvette filled with PB of desired molarity was placed at 42 or 52 °C for 10 min; thereafter, an aliquot (15–100 μl) of a stock CP solution preheated at 35 °C was added and thoroughly stirred with the buffer for 15 s (measurement dead time). The final volume of the mixture was 1 ml in 0.5 cm cuvettes or 2 ml in 1 cm cuvettes. The kinetics of turbidity changes were monitored at 313 nm (Specord) or 320 nm (Aminco).

The initial rate of aggregation (v_0^{agg}) was calculated in absorbance units/min from the initial linear portion of the kinetic curve. The pseudo-first-order rate constants (k_I) for aggregation were determined using the following equation (Kurganov, 2002a,b; Kurganov et al., 2002):

$$A = A_{lim}\{1 - \exp[-k_I(t - t_0)]\}, \quad (1)$$

where t is the time, A the turbidity (absorption at 320 nm), A_{lim} the limiting value of A at $t \to \infty$ and t_0 corresponds to $A = 0$.

The ionic strength (μ) was calculated as:

$$\mu = \frac{1}{2}\sum c_i z_i^2, \quad (2)$$

where z_i and c_i are ion molal concentrations and charges, respectively (Avery, 1982).

2.3. CD spectroscopy

The CD spectra of the TMV protein were recorded between 198 and 250 nm using a modified Mark V dichrograph (Jobin-Ivon, France) as described previously (Orlov et al., 2001). The kinetics of TMV CP denaturation at 42 °C were recorded at 215 nm. Specifically, a 0.5 cm cuvette (assay volume of 1 ml) was filled with 30 mM PB (pH 8.0) and placed at 42 °C for

10 min. Thereupon, the CP was added to a final concentration of 100 μg/ml to the cuvette. Prior to recording the CD signal, the mixture was stirred for 15 s (dead time).

2.4. Fluorescence measurements

Spectral and kinetic fluorescence intensity measurements were taken using a Hitachi MPF-4 spectrofluorimeter (Japan) in 1 cm cuvettes. Fluorescence from 100 μg/ml TMV CP in 30 mM PB (pH 8.0) was excited at 280 nm; the emission spectra were recorded between 300 and 400 nm. The measurement temperature was varied in a stepwise manner. The kinetics of denaturation were recorded at the emission wavelength of 320 nm under the same conditions that were used in CD measurements at 215 nm.

3. Results and discussion

3.1. Effects of pH and ionic strength on "nonspecific" TMV CP aggregation

In the first series of experiments, we studied how the rate of macroscopic TMV CP aggregation varied with pH. It is well known (Butler, 1984) that the type of specific ordered aggregates formed by the TMV CP in a solution depends on the pH of that solution. At pH values in the range from 7.5 to 9.0 and ionic strengths in the range from 10 to 100 mM, the TMV CP exists as a dynamic mixture of pentamers and trimers, with a minor amount of monomers. This mixture is known as the A- or 4S-protein. At pH of about 7.0 and ionic strength of about 100 mM, 60−80% of the TMV CP is in the form of the 20S-aggregate (two-layer disk or short helix), with the other 20–40% being the 4S-protein. At pH ≤6.0, long virus-like helical aggregates are formed called the repolymerized protein (Butler, 1984). The effect of pH on the rate of heating-induced macroscopic TMV CP aggregation was studied using turbidimetry. Specifically, aggregation was monitored by continuously recording the absorption at 313 or 320 nm.

Fig. 1 shows how the absorption of 133 μg/ml TMV CP in 50 mM PB at 313 nm (A_{313}) varied with time at 52 °C for different pH values. It can be seen that the initial rate of nonspecific TMV CP aggregation (v_0^{agg}) increases less than fourfold as the pH is raised from 6.3 to 8.8 (Fig. 1, curves 1–4).

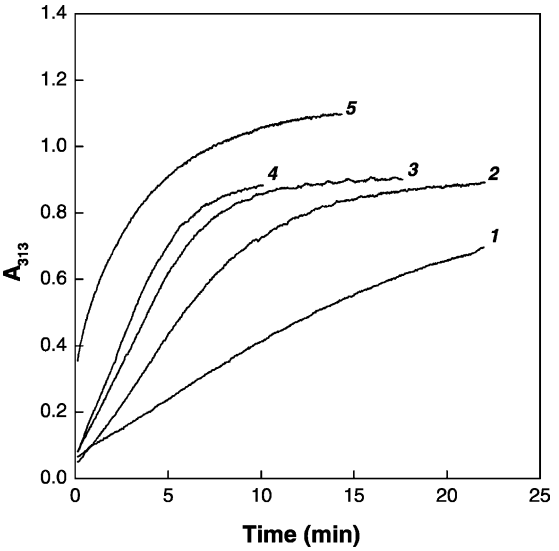

Fig. 1. Effect of pH on TMV CP macroscopic aggregation at 52 °C, as assessed from absorption of 133 μg/ml TMV CP in 50 mM PB at 313 nm (A_{313}): (1) pH 6.3; (2) pH 7.0; (3) pH 8.1; (4) pH 8.8; (5) pH 5.6.

At pH 5.6, optimal for CP repolymerization into the helical form, the rate of CP aggregation significantly increased and the shape of the turbidity curve changed (Fig. 1, curve 5). Supposedly, virus-like helical TMV CP polymers formed macroscopic aggregates by a mechanism different from that involved in nonspecific aggregation of small (4S and 20S) polymers. Note, however, that the above-mentioned pH dependence of specific TMV CP aggregation (polymerization) reported by Butler (1984) was obtained at room temperature; therefore, the polymerization state of the protein at 52 °C in the absence of nonspecific aggregation remains unknown.

In our previous study (Orlov et al., 2001), the rate of macroscopic TMV CP aggregation was found to be strikingly sensitive to solution ionic strength. In the present study, we analyzed the data using a pseudo-first-order kinetic model (Kurganov et al., 2002). This analysis showed that, at 52 °C, the rate constant k_I satisfied the positive well-known Bronsted relationship ($\ln k_I \sim \sqrt{\mu}$) over a range of PB molarities from 20 to 70 mM (Fig. 2). It is noteworthy that the Bronsted plot constructed from the data of

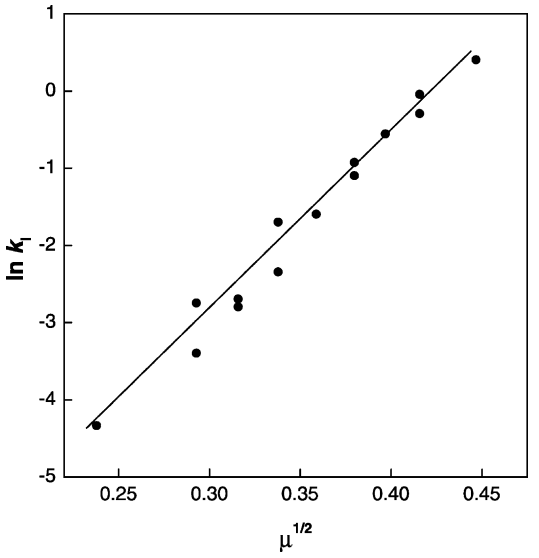

Fig. 2. Plots of the pseudo-first-order rate constant k_I for TMV CP aggregation at 52 °C vs. ionic strength, as determined at the protein concentration of 50 μg/ml in PB (pH 8.0). The k_I values (min^{-1}) and ionic strengths were calculated as described in Section 2.2.

these experiments had a much steeper slope than the slopes of such plots for reactions between simple ions (Avery, 1982). The steep slope suggests that repulsive electrostatic interactions between negatively charged TMV CP subunits strongly inhibit heating-induced macroscopic aggregation of this protein. Neutralization of its charge at high ionic strengths results in very large increase in the aggregation rates and final size of aggregates. Therefore, it is likely that, amorphous TMV CP aggregation is driven by hydrophobic forces. The remarkable sensitivity of the rate of nonspecific TMV CP aggregation to ionic strength testifies to a rather delicate balance between strong repulsive electrostatic interactions and strong attractive hydrophobic interactions on the surfaces of TMV CP molecules. An inverse correlation between the rates of protein aggregation and their overall net charge was reported recently in a study from Prof. C.M. Dobson's laboratory (Chiti et al., 2002).

3.2. Kinetics of partial denaturation of the TMV CP

A vast literature describing aggregation of different proteins has accumulated in recent years. In most studies, aggregation is recorded using turbidimetric techniques. Many of these studies report that proteins start to aggregate following some lag (Fink, 1998). We tested a variety of conditions, but in no case did any lag period precede macroscopic TMV CP aggregation. Its initial rate was always the maximal one (Orlov et al., 2001). To explore possible reasons of this peculiarity, we studied the kinetics of thermal denaturation of the TMV CP under conditions favoring its nonspecific aggregation.

As shown in our previous study (Orlov et al., 2001), irreversible macroscopic aggregates are formed by partially unfolded TMV CP molecules. These molecules are completely denatured as judged by differential scanning calorimetry and CD spectroscopy in the so-called aromatic region (250–300 nm), but retain more than half of their initial secondary structure, as can be judged from the far-UV CD spectra (200–250 nm) (Orlov et al., 2001). Heating-induced nonspecific TMV CP aggregation is quite remarkable in that its rate is easy to control by changing the protein concentration, solution ionic strength, and temperature.

Therefore, the conditions for measuring the kinetics of partial thermal denaturation of the TMV CP by CD spectroscopy (i.e. the kinetics of its transition from the native form with $[\Theta]_{208} = -16{,}300^\circ\ cm^2/dmol$ to a form with $[\Theta]_{208} = -10{,}000^\circ\ cm^2/dmol$ (Orlov et al., 2001) were chosen so as to deal with the process not too fast to follow it by a decrease in the negative $[\Theta]_{215}$ value but more rapid than the formation of highly scattering large aggregates. Specifically, the kinetics of denaturation of 100 μg/ml CP in 30 mM PB (pH 8.0) at 42 °C were recorded at 215 nm, the wavelength at which the difference between the ellipticity values for the native and partially denatured forms of the protein is close to its maximum while the contribution from the absorption of the protein is still not too high. For the native form of the TMV CP, $[\Theta]_{215} = -15{,}100^\circ\ cm^2/dmol$. To allow for rapid mixing, we used cuvettes with a path length of ≥0.5 cm; the stirring-related dead time was 15 s.

The results are shown in Fig. 3. Immediately after the dead time, $[\Theta]_{215}$ is $-12{,}600^\circ\ cm^2/dmol$; over the subsequent 4 min, it declines to about $-9600^\circ\ cm^2/dmol$ (the end of partial denaturation), leveling off thereafter. These data suggest that $[\Theta]_{215}$ drops by half within the first 15 s at 42 °C (during stirring).

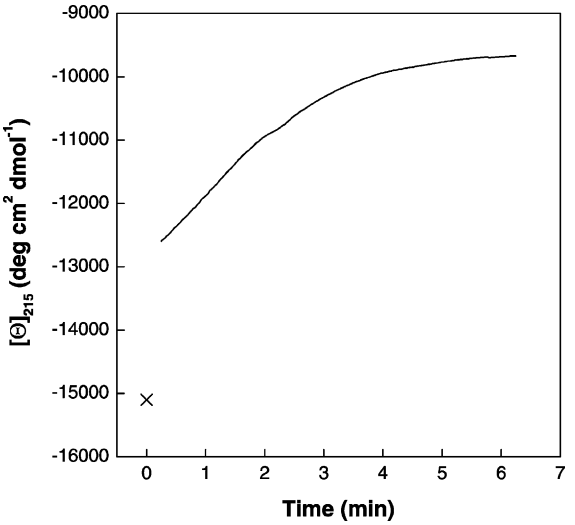

Fig. 3. Kinetics of TMV CP denaturation at 42 °C, as assessed by CD spectroscopy at 215 nm. CP concentration, 100 μg/ml; PB (pH 8.0), 30 mM.

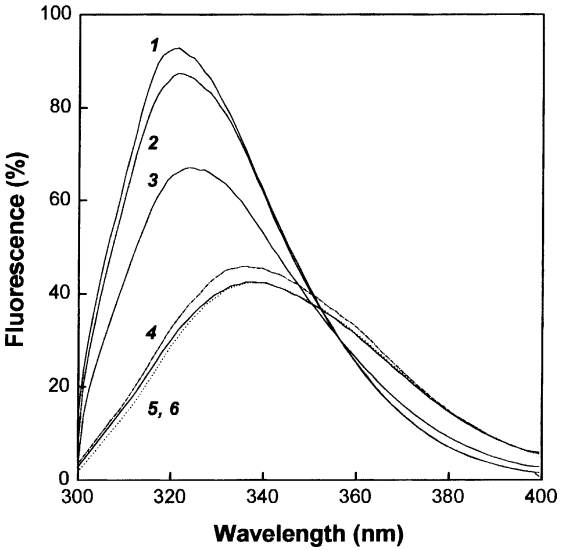

Fig. 4. Effect of temperature on the intrinsic fluorescence spectrum of the TMV CP. CP (100 μg/ml) in 30 mM PB (pH 8.0) was stepwise heated for 15 min at each of the temperatures indicated: (1) 25 °C; (2) 32 °C; (3) 38 °C; (4) 42 °C; (5) 49 °C; (6) 56 °C.

To test this suggestion, the kinetics of denaturation of the TMV CP at 42 °C were monitored from changes in its intrinsic fluorescence at 320 nm (I_{320}). The experimental conditions were the same as in the CD experiments: 100 μg/ml CP in 30 mM PB (pH 8.0). Fluorescence-registered thermal denaturation of the TMV CP is known to proceed in one stage (Taniguchi & Taniguchi, 1975) and is associated with a large decrease in I_{320} (Fig. 4). The denaturation temperature of the TMV CP at which the total I_{320} declines by half was determined to be 42 °C, which is close to the denaturation temperature (~41 °C) estimated by differential scanning calorimetry under similar conditions (200 μg/ml CP in 30 mM PB; pH 8.0 (Orlov et al., 2001)).

Fig. 5 shows how I_{320} decreases during TMV CP denaturation. The data are presented relative to the total decrease in I_{320} (taken as 100%). The $[\Theta]_{215}$ data redrawn in relative units from Fig. 3 are shown for comparison. The initial extent of denaturation turned out to be similar with the two methods: 45%, with the CD; and 50%, with the fluorescence spectroscopy. However, thereafter $[\Theta]_{215}$ changed significantly more slowly than I_{320} (Fig. 5). These data suggest that partial denaturation of the TMV CP at 42 °C proceeds in at least two stages. At the first stage, which is over in less than 15 s, the TMV CP passes from the native

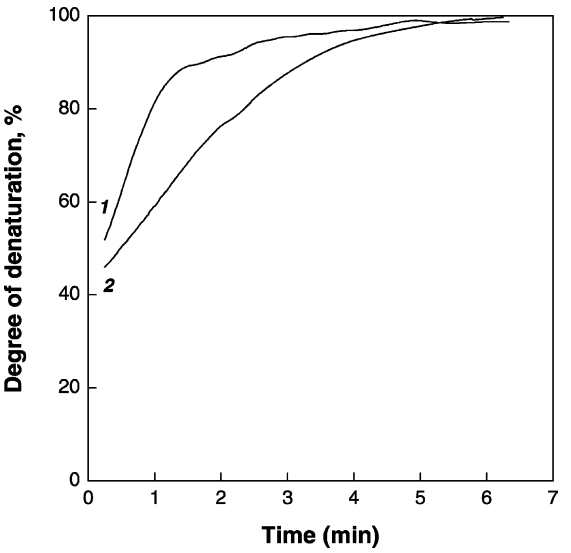

Fig. 5. I_{320} (1) and $[\Theta]_{215}$ (2) profiles for TMV CP denaturation at 42 °C. Both quantities are given relative to their respective total change taken as 100%. CP concentration, 100 μg/ml; PB (pH 8.0), 30 mM.

"−15,100°" form to the "−12,600°" form. The second stage, which lasts for about 4 min, corresponds to a transition from the "−12,600°" form to a highly stable "−9600°" form. This form is completely disordered as judged by differential scanning calorimetry (Orlov et al., 1998, 2001), aromatic CD (Orlov et al., 2001) and fluorescence spectroscopy (Orlov et al., 1998, 2001; see also Fig. 4), but preserves its far-UV CD spectrum even after heating to 80° (Orlov et al., 2001).

Changes in the $[\Theta]_{215}$ value signify disordering the native secondary structure, which in the TMV CP is represented nearly entirely by α-helical elements. These α-helices are located in the segment of the CP molecule, which in the TMV CP virions occupied position at low radius, close to the virion axis (Bhyravbhatla, Watowich, & Caspar, 1998; Namba, Pattanayek, & Stubbs, 1989; see also Fig. 7). Changes in the I_{320} reflect alterations in the native environment of Trp and Tyr residues, which in CP subunits in TMV virions lie at radius >6.5 nm from the axis, not far from the virion outer surface. Hence, the two methods yield different results because they furnish information on the rate and extent of disordering in different regions of the TMV CP subunit. At neutral pH values, the rate of the TMV CP thermal denaturation depends only slightly on the ionic strength (Kurganov et al., 2002; Orlov et al., 1998) and at high ionic strengths, macroscopic TMV CP aggregation proceeds very rapidly (Fig. 2; see also Kurganov et al., 2002; Orlov et al., 2001). It looks as if unfolding of only a small high-radius part of a TMV CP molecule is sufficient for its transition to nonspecific aggregation-prone state.

Thus, the reason for very rapid (without any lag period) heating-induced amorphous TMV CP aggregation may be a very fast transition of the CP molecules to a slightly unfolded state and a high affinity of hydrophobic patches of these slightly unfolded molecules for one other.

3.3. Macroscopic aggregation of coat proteins of other helical viruses

The propensity of the TMV CP to undergo nonspecific aggregation raises the question of whether this property is unique to this protein or may occur in CPs of other helical plant viruses. To answer this question, we experimented with CPs of a ts21–66 mutant of wild-type TMV strain U1, rod-like ToMV, and flexuous PVX. Specifically, we recorded the "melting curves" for these proteins under conditions previously employed in the experiments with the wild-type TMV CP (U1 CP hereafter) (Abu-Eid et al., 1994; Kurganov et al., 2002; Orlov et al., 2001). The ts21–66 CP has two amino acid substitutions (Ile 21 → Thr, Asp 66 → Gly) (Dobrov et al., 1997); the ToMV is closely related to TMV strain U1 (their CPs differ in 26 amino acids more or less evenly distributed along the polypeptide chain (Goelet et al., 1982; Ohno et al., 1984)), and the PVX CP is unrelated to the TMV CP in the primary structure (Skryabin et al., 1988).

Fig. 6 shows the A_{313} versus temperature curves for stepwise heating of U1, ts21–66, ToMV, and PVX CPs in 50 mM PB (pH 7.0). Compared with the U1 CP, the ts21–66 CP undergoes nonspecific aggregation at somewhat lower temperatures. The temperature of half-maximal increase in A_{313} ($T_{0.5}^{agg}$) was 37 °C for the ts21–66 CP and 43.5 °C for the U1 CP (see also Abu-Eid et al., 1994). The lower $T_{0.5}^{agg}$ value for the mutant CP may be due to general destabilization of its structure resulting from two amino acid substitutions mentioned above (Dobrov et al., 1997). This result provides further support for the conclusion (Orlov et al., 2001) that partial unfolding

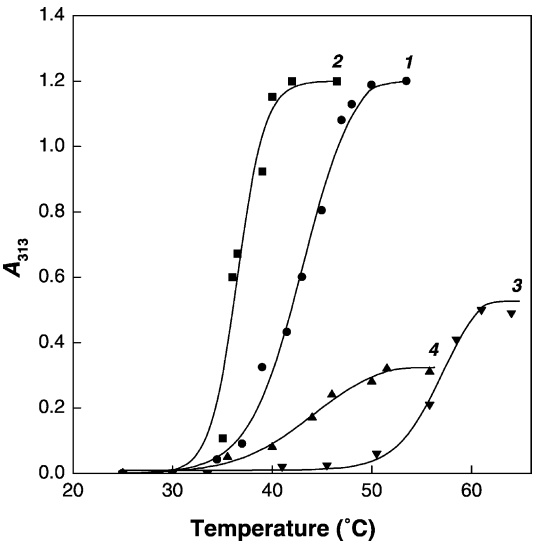

Fig. 6. Stepwise heating of (1) wild-type TMV, (2) ts21–66, (3) ToMV, and (4) PVX CPs. CP (200 μg/ml) was stepwise heated for 15 min in 50 mM PB (pH 7.0).

is responsible for the nonspecific aggregation of the TMV CP. The ts21–66 CP did not differ from the U1 CP in the final turbidity level (Fig. 6, curves 1 and 2).

The ToMV CP also readily underwent nonspecific aggregation on heating, but at temperatures much higher than those required for U1 CP aggregation (Fig. 6, curve 3). The $T_{0.5}^{agg}$ for the ToMV CP was estimated at 57 °C. The final turbidity level observed before coagulation was significantly lower for the ToMV CP than for the U1 or the ts21–66 CP (0.5 absorbance units/cm versus 1.3 absorbance units/cm), suggesting that for the ToMV CP the maximal size of aggregates still remaining in suspension is much smaller than that for TMV CP.

From analysis of the melting curves for CP preparations isolated from flexuous PVX virions, the $T_{0.5}^{agg}$ was estimated at 47 °C (Fig. 6, curve 4), which compares to 43.5 °C for the U1 CP. However, the A_{313max} was as low as ~0.35 absorbance units/cm. This value is three- to fourfold lower than for TMV CP.

The most spectacular difference between the TMV and PVX CPs was observed in their responses to changes in solution ionic strength. As mentioned above (Orlov et al., 2001; see also Fig. 2), the rate of heating-induced macroscopic TMV CP aggregation is extremely sensitive to ionic strength: the initial rate of aggregation increases by almost an order of magnitude for every 10 mM increase in PB molarity in the range from 20 to 50 mM. Nothing of the kind was observed with the PVX CP (Table 1). We prepared 200 μg/ml PVX CP in PBs (pH 7.0) of different molarities and recorded its aggregation at 52 °C for each molarity. In 10 mM PB, a moderate extent of PVX CP aggregation was observed, whereas the TMV CP did not aggregate. In 25 mM PB, the initial rate v_0^{agg} of PVX CP aggregation was 14 times higher than that of TMV CP aggregation. However, in 50 mM PB, the initial rate of TMV CP aggregation was threefold higher than the rate of PVX CP aggregation. In 75 mM PB, the difference grew, becoming as great as 22 times. In 100 mM PB, this difference became 48 times. With an increase in the buffer molarity from 10 to 50 mM, the initial rate of PVX CP aggregation rose only sixfold and stopped rising at higher ionic strengths (Table 1). As mentioned above, strong electrostatic repulsion between TMV CP subunits was suggested to be in a delicate balance with strong hydrophobic attraction. Obviously, no such balance can be suggested for PVX CP molecules.

Table 1
The initial rate of aggregation (v_0^{agg}) as a function of solution ionic strength for TMV and PVX coat proteins

Protein	Phosphate buffer molarity				
	10 mM	25 mM	50 mM	75 mM	100 mM
TMV CP	<0.0002	0.0035	0.18	1.42	3.15
PVX CP	0.0095	0.0475	0.063	0.065	0.066

v_0^{agg} (absorbance units/min) was calculated as described in Section 2.2. The data for the TMV CP were recalculated from Orlov et al. (2001). The rate of PVX CP aggregation was measured at 52 °C and the protein concentration of 200 μg/ml in PB (pH 7.0) of indicated molarities.

The initial rates of aggregation of CPs of closely related ToMV and TMV similarly depended on the protein concentration and the ionic strength (data not shown).

Since the early X-ray diffraction studies with a sufficiently high resolution of 0.3–0.4 nm, it has become evident that TMV CP subunits differ from molecules of other globular proteins in the presence of large hydrophobic patches on their surfaces (Bloomer, Champness, Bricogne, Staden, & Klug, 1978; Stubbs, Warren, & Holmes, 1977). These hydrophobic patches serve as stabilization factors in very strong interactions between subunits in ordered supramolecular TMV CP aggregates of both helical (virion-like) and cylindrical (20S disk-like) types (Bhyravbhatla et al., 1998; Namba et al., 1989). It is these hydrophobic patches that account for the propensity of the TMV CP to rapidly form very large nonspecific aggregates upon neutralization of strong electrostatic repulsion between its subunits at high ionic strengths.

The results obtained suggest that the first stage of thermal denaturation of the TMV CP is unfolding of a region lying in virions and 20S disks at radius of 6.5–9 nm. This stage proceeds very quickly. As a result, TMV CP subunits acquire a propensity to undergo rapid nonspecific aggregation.

This external layer (6.5–9 nm from the axis) of the TMV CP molecule is enriched in hydrophobic residues (including Trp and Tyr), which are involved into the intersubunit interactions in TMV virions or disks, forming the so-called “hydrophobic girdle” (Bloomer et al., 1978), a ribbon of hydrophobic residues running from subunit to subunit through the entire virion

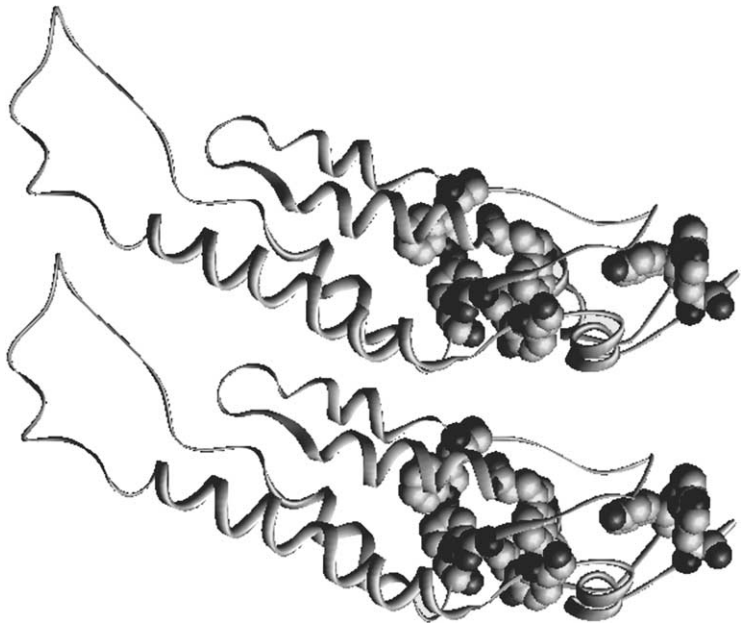

Fig. 7. Side-view of the structure of two TMV CP subunits in the virion. The virion axis is on the left. Tyrosine and tryptophan residues are highlighted. This figure was generated from the X-ray diffraction data (Namba et al., 1989) using the WebLab ViewerLite© program.

and 20S disks and imparting stability to them. Supposedly, disordering of this girdle is responsible for the aberrant hydrophobic interaction between subunits (Fink, 1998; Wetzel, 1994) that initiates TMV CP macroscopic aggregation. Being conserved in the ToMV (Wang, Planchart, & Stubbs, 1998), the hydrophobic girdle is unlikely to be present in the PVX.

At the second stage of thermal denaturation of the TMV CP (up to 4 min at 42 °C), about half of the four-helix α-helical bundle, which constitutes the core of its structure, unfolds (Bhyravbhatla et al., 1998; Namba et al., 1989; see also Fig. 7). The other half of the helical bundle is stable against heat stress and does not unfold even at 80 °C (Orlov et al., 2001). It is likely that CP molecules with partly unfolded α-helices can also form macroscopic aggregates. Their aggregation may contribute to the unusually high heat stability of the remaining α-helical elements of TMV CP subunits.

Acknowledgements

We thank Dr. V.K. Novikov for supplying ToMV CP preparations and Dr. A.A. Rosenkranz for useful suggestions. This work was supported by the Russian Foundation for Basic Research (grants nos. 02-04-48704, 02-04-48842, and 00-15-97787), and Program “Physico-Chemical Biology”.

References

Abu-Eid, M. M., Kust, S. V., Makeeva, I. V., Novikov, V. K., & Dobrov, E. N. (1994). Study of thermal aggregation of several tobamoviruses coat proteins. *Molekuliarnaia Genetika, Mikrobiologiia i Virusologiia*, *3*, 28–32.

Arutyunyan, A. M., Rafikova, E. R., Drachev, V. A., & Dobrov, E. N. (2001). Appearance of “β-like” circular dichroism spectra on protein aggregation that is not accompanied by transition to β-structure. *Biochemistry (Moscow)*, *66*, 1378–1380.

Avery, H. E. (1982). *Basic reaction kinetics and mechanisms*. London: Macmillan.

Bhyravbhatla, B., Watowich, S. J., & Caspar, D. L. (1998). Refined atomic model of the four-layer aggregate of the tobacco mosaic virus coat protein at 2.4 Å resolution. *Biophysical Journal*, *74*, 604–615.

Bloomer, A. C., Champness, J. N., Bricogne, G., Staden, K., & Klug, A. (1978). Protein disk of tobacco mosaic virus at 2.8 Å resolution within and between subunits. *Nature*, *276*, 362–368.

Bucciantini, M., Giannoni, E., Chiti, F., Baroni, F., Formigli, L., Zurdo, J., Taddei, N., Ramponi, G., Dobson, C. M., & Stefani, M. (2002). Inherent toxicity of aggregates implies a common

mechanism for protein misfolding diseases. *Nature, 416*, 507–511.

Butler, P. J. G. (1984). The current picture of the structure and assembly of tobacco mosaic virus. *The Journal of General Virology*, *65*, 253–279.

Chiti, F., Calamai, M., Taddei, N., Stefani, M., Ramponi, G., & Dobson, C. M. (2002). Studies of the aggregation of mutant proteins in vitro provide insights into the genetics of amyloid diseases. *Proceedings of the National Academy of Sciences of the United States of America*, *99*(Suppl. 4), 16419–16426.

Chiti, F., Webster, P., Taddei, N., Clark, A., Stefani, M., Ramponi, G., & Dobson, C. M. (1999). Designing conditions for in vitro formation of amyloid protofilaments and fibrils. *Proceedings of the National Academy of Sciences of the United States of America*, *96*, 3590–3594.

Conway, K. A., Lee, S. J., Rochet, J. C., Ding, T. T., Williamson, R. E., & Lansbury Jr., P. T. (2000). Acceleration of oligomerization, not fibrillization, is a shared property of both α-synuclein mutations linked to early-onset Parkinson's disease: implications for pathogenesis and therapy. *Proceedings of the National Academy of Sciences of the United States of America*, *97*, 571–576.

Dobrov, E. N., Abu-Eid, M. M., Solovyev, A. G., Kust, S. V., & Novikov, V. K. (1997). Properties of the coat protein of a new tobacco mosaic virus coat protein ts-mutant. *Journal of Protein Chemistry*, *16*, 27–36.

Fandrich, M., Fletcher, M. A., & Dobson, C. M. (2001). Amyloid fibrils from muscle myoglobin. *Nature*, *410*, 165–166.

Fink, A. L. (1998). Protein aggregation: folding aggregates, inclusion bodies and amyloid. *Structure with Folding & Design*, *3*, R9–R23.

Fraenkel-Conrat, H. (1957). Degradation of tobacco mosaic virus with acetic acid. *Virology*, *1*, 1–4.

Ganesh, C., Zaidi, F. N., Udgaonkar, J. B., & Varadarajan, R. (2001). Reversible formation of on-pathway macroscopic aggregates during the folding of maltose binding protein. *Protein Science*, *10*, 1635–1644.

Goelet, P., Lomonossoff, G. P., Butler, P. J., Akam, M. E., Gait, M. J., & Karn, J. (1982). Nucleotide sequence of tobacco mosaic virus RNA. *Proceedings of the National Academy of Sciences of the United States of America*, *79*, 5818–5822.

Goldshtein, M. I., Grebenshcikov, N. I., Kust, S. V., Kaftanova, A. S., Dobrov, E. N., & Atabekov, I. G. (1990). Effect of proteolytic cleavage of potato virus X coat protein on the protein ability to self-assemble with the viral RNA and on the viral infectivity. *Molekuliarnaia Genetika, Mikrobiologiia i Virusologiia*, *2*, 9–16.

Goodman, R. M. (1975). Reconstitution of potato virus X in vitro. I. Properties of the dissociated protein structural subunits. *Virology*, *68*, 287–298.

Guijarro, J. I., Sunde, M., Jones, J. A., Campbell, I. D., & Dobson, C. M. (1998). Amyloid fibril formation by an SH3 domain. *Proceedings of the National Academy of Sciences of the United States of America*, *95*, 4224–4228.

Hartley, D. M., Walsh, D. M., Ye, C. P., Diehl, T., Vasquez, S., Vassilev, P. M., Teplow, D. B., & Selkoe, D. J. (1999). Protofibrillar intermediates of amyloid β-protein induce acute electrophysiological changes and progressive neurotoxicity in cortical neurons. *Journal of Neuroscience*, *19*, 8876–8884.

Kopito, R. R. (2000). Aggresomes, inclusion bodies and protein aggregation. *Trends in Cell Biology*, *10*, 524–530.

Kurganov, B. I. (2002a). Principles of quantitative estimation of the chaperone-like activity. *Tsinghua Science and Technology*, *7*, 331–339.

Kurganov, B. I. (2002b). Estimation of molecular chaperone activity in test-systems based on protein aggregation suppression. *Uspekhi Biokhimii*, *42*, 89–138 (in Russian).

Kurganov, B. I., Rafikova, E. R., & Dobrov, E. N. (2002). Kinetics of thermal aggregation of tobacco mosaic virus coat protein. *Biochemistry (Moscow)*, *67*, 525–533.

Lambert, M. P., Barlow, A. K., Chromy, B. A., Edwards, C., Freed, R., Liosatos, M., Morgan, T. E., Rozovsky, I., Trommer, B., Viola, K. L., Wals, P., Zhang, C., Finch, C. E., Krafft, G. A., & Klein, W. L. (1998). Diffusible, nonfibrillar ligands derived from Aβ1–42 are potent central nervous system neurotoxins. *Proceedings of the National Academy of Sciences of the United States of America*, *95*, 6448–6453.

Namba, K., Pattanayek, R., & Stubbs, G. (1989). Visualization of protein-nucleic acid interactions in a virus. Refined structure of intact tobacco mosaic virus at 2.9 Å resolution by X-ray fiber diffraction. *Journal of Molecular Biology*, *208*, 307–325.

Ohno, T., Aoyagi, M., Yamanashi, Y., Saito, H., Ikawa, S., Meshi, T., & Okada, Y. (1984). Nucleotide sequence of the tobacco mosaic virus (tomato strain) genome and comparison with the common strain genome. *Journal of Biochemistry (Tokyo)*, *96*, 1915–1923.

Orlov, V. N., Arutyunyan, A. M., Kust, S. V., Litmanovich, E. A., Drachev, V. A., & Dobrov, E. N. (2001). Macroscopic aggregation of tobacco mosaic virus coat protein. *Biochemistry (Moscow)*, *66*, 154–162.

Orlov, V. N., Kust, S. V., Kalmykov, P. V., Krivosheev, V. P., Dobrov, E. N., & Drachev, V. A. (1998). A comparative differential scanning calorimetric study of tobacco mosaic virus and of its coat protein ts mutant. *FEBS Letters*, *433*, 307–311.

Skryabin, K. G., Kraev, A. S., Morozov, S. Y., Rozanov, M. N., Chernov, B. K., Lukasheva, L. I., & Atabekov, J. G. (1988). The nucleotide sequence of potato virus X RNA. *Nucleic Acids Research*, *16*, 10929–10930.

Stubbs, G., Warren, S., & Holmes, K. (1977). Structure of RNA and RNA binding site in tobacco mosaic virus from 4 Å map calculated from X-ray fibre diagrams. *Nature*, *267*, 216–221.

Taniguchi, M., & Taniguchi, T. (1975). Thermally induced conformational changes of tobacco mosaic virus and their protein assemblies. *Biochimica et Biophysica Acta*, *386*, 1–17.

Wang, H., Planchart, A., & Stubbs, G. (1998). Caspar carboxylates: the structural basis of tobamovirus disassembly. *Biophysical Journal*, *74*, 633–638.

Wetzel, R. (1994). Mutations and off-pathway aggregation of proteins. *Trends in Biotechnology*, *12*, 193–198.